




Design and analysis of a compact ultrathin penta-band metamaterial absorber

ASHA VERMA* and OM PRAKASH MEENA

Department of Electronics and Communication Engineering, Maulana Azad National Institute of Technology, Bhopal 462003, India
e-mail: asha.nit123@gmail.com

MS received 24 May 2023; revised 19 September 2023; accepted 4 October 2023

Abstract. This study proposes a novel penta-band metamaterial absorber (PMA) that consists of an asymmetric dual split square metal resonator (DSSR), a dielectric substrate, and a copper metal-based ground plane. The design of the PMA unit cell is relatively compact and ultrathin for various penta-band applications. This work asserts a unit cell of 5×5 mm² area and 1 mm thick substrate. The EM properties of the proposed metamaterial absorber were simulated in ANSYS HFSS software and compared with the experimental results obtained from Vector Network Analyzer post-fabrication of unit cell PMA. The relative error attained between simulated and experimental findings was less than 2%. The pentamerous absorption peaks of nearly perfect absorption were found specifically at 10.40, 12.80, 21.05, 24.29, and 30.41 GHz frequencies with the absorptivity ratios of almost 99.99%, 98.44%, 86.78%, 92.74%, and 93.65%, respectively.

Keywords. Multi-band absorber; penta-band; metamaterial absorber; HFSS; dual split square metal resonator (DSSR).

1. Introduction

The introduction of a metamaterial into the communication systems is a potential solution to reduce the impact of EM waves [1]. Metamaterial is a specific kind of material that is designed to efficiently absorb EM radiation and shows uncommon properties, which also permits their use in different applications such as Specific Absorption Rate (SAR) reduction [2], superconductor [3], superlens imaging [4], tunable metamaterial [5], antenna [6], and absorber [7], etc.

Metamaterial absorbers (MA) could be designed to effectively absorb EM radiations at infrared, visible, and microwave frequencies [8, 9]. In the microwave domain, various resonator structures have been proposed for multi-band applications. A Summarised review of the proposed MA with different multi-band metamaterial absorbers is shown in table 4. Multi-band MAs are able to show perfect absorption at various discrete frequency peaks, whereas single-band MAs stick only a single frequency band; that is why multi-band MAs are preferable to single-band MAs. There are very limited pieces of literature available that present pentaband metamaterial absorbers with high absorptivity. Recently, a pentaband metamaterial absorber has been designed with four fold resonator having absorption peaks of 99.59, 95.49, 97.5, 99.25, and 93.29%,

respectively, at 3.35, 5.1, 9.5, 11.55, and 16.9 GHz by Garg *et al* [10]. This design consists of a 1 mm substrate thickness and 10 mm \times 10 mm unit cell area. This motivates the presented research work to investigate the design of the metamaterial absorber structure so that it can be efficiently applied for multi-resonance bands while maintaining a compact size.

The proposed work has been carefully designed with a compact size of 5 mm \times 5 mm and substrate thickness of 1 mm for a pentaband metamaterial absorber with good absorptivity. Considering various applications such as sensors, military radar, stealth devices, etc.

This research work proposes a novel, cost-effective, simply-structured, compact, and ultrathin metamaterial absorber for pentaband applications in the microwave region. The design of the proposed metamaterial absorber consists of an asymmetric dual-split square metal resonator (DSSR), a dielectric substrate, and a copper metal-based ground plane. Five bands are formed by combining two compact geometries onto a single structure. The simulation results showed that the pentamerous absorption peaks of nearly perfect absorption were explicitly found at 10.40, 12.80, 21.05, 24.29, and 30.41 GHz frequencies with ratios of almost 99.99%, 98.44%, 86.78%, 92.74%, and 93.65% absorptivity, respectively. Summarized results for the proposed MA are also presented in table 4. The prototype with 50 mm \times 50 mm was also fabricated in the laboratory, and metamaterial absorber properties were

*For correspondence

experimentally investigated using a Vector network analyzer.

2. Design and Modelling

The unit cell structure of the absorber is shown in figure 1. The top layer of the absorber is an asymmetric dual-split square metal resonator (DSSR) made of copper (conductivity, $\sigma = 5.8 \times 10^8$ S/m), which is the main design component of the presented absorber. The proposed DSSR layer configuration is a combination of two geometries, *i.e.*, inner split square (SSR)_i, and outer split square ring (SSR)_o, shown as Design I and II, respectively, in figure 2. Both SSRs have two splits of length 0.4 mm and width 0.2 mm. The top view of the proposed unit cell configuration is also shown in Design III of figure 2. The second layer, above which DSSR is centered, is an FR4 dielectric substrate of unit area 5 mm × 5 mm, having a permittivity (ϵ_r) of 4.3 and loss tangent ($\tan \delta$) of 0.025. FR4 substrate has been used due to its low cost, great mechanical strength, and higher electrical insulation [11]. Both the top and bottom layers are 0.035 mm thin, whereas the substrate layer is 1 mm thick, allowing the absorber to be ultrathin. The proposed design works on the principle of resonance. The absorption rate (*A*) of an absorber can be defined as:

$$A = 1 - |S_{11}|^2 - |S_{21}|^2 \tag{1}$$

where $|S_{11}|$ and $|S_{21}|$ is defined as reflection and transmission coefficients, respectively. In a perfect scenario of

100% absorption, S_{21} and S_{11} should be equal to zero (table 1).

In the proposed absorber, transmission coefficient $S_{21} \sim 0$ and absorptivity depends only on the reflected electromagnetic wave. The absorption rate is represented as:

$$A = 1 - |S_{11}|^2 \tag{2}$$

Therefore, in order to get near unity absorption, the power reflected from the unit cell needs to be lowered as much as possible.

3. Results and discussion

All three geometries (SSR)_i, (SSR)_o, and DSSR are simulated, and results are obtained in figure 3, figure 4 and figure 5, respectively. These figures show the absorption peaks with different resonance frequencies and the effect of each geometry in terms of absorptivity. Table 2 represents the effectiveness of (SSR)_i and (SSR)_o on unit cell design. In contrast, table 3 shows the five resonant bands and the absorptivity at these bands.

3.1 Simulation studies

This proposed design implemented in 0-35 GHz works on the principle of Maxwell's equation. This design consists of a floquet port which is related to a wave port in the set of modes. Boundary condition plays a very important role here.

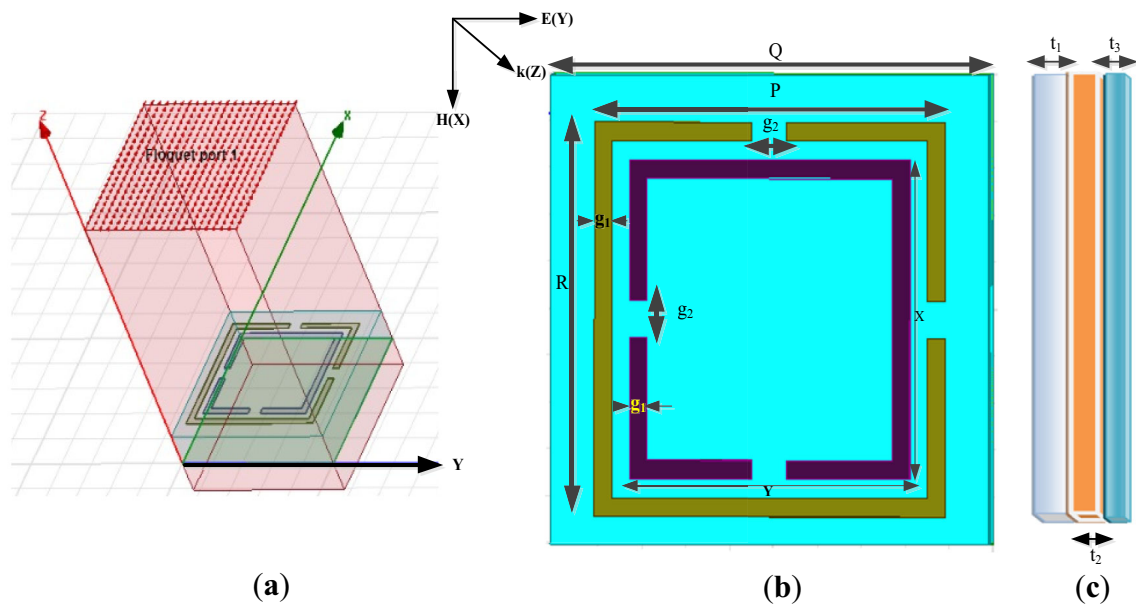


Figure 1. Illustration of (a) Simulation set up of unit cell in HFSS, (b) front view, and (c) side view of unit cell's structure layout.

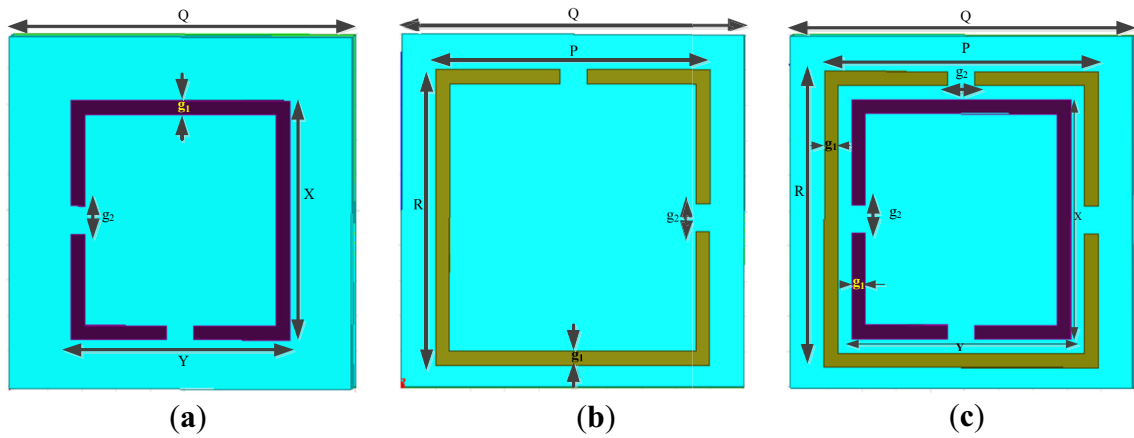


Figure 2. Top view of unit cell geometry (a) Design I – (SSR)_i, (b) Design II – (SSR)_o, and (c) Design III - proposed DSSR.

Table 1. Unit cell structure geometry.

Parameters	Q	P	R	X	Y	g ₁	g ₂	t ₁	t ₂	t ₃
Value (mm)	5	4	4.2	3.2	3.4	0.2	0.4	0.035	1	0.035

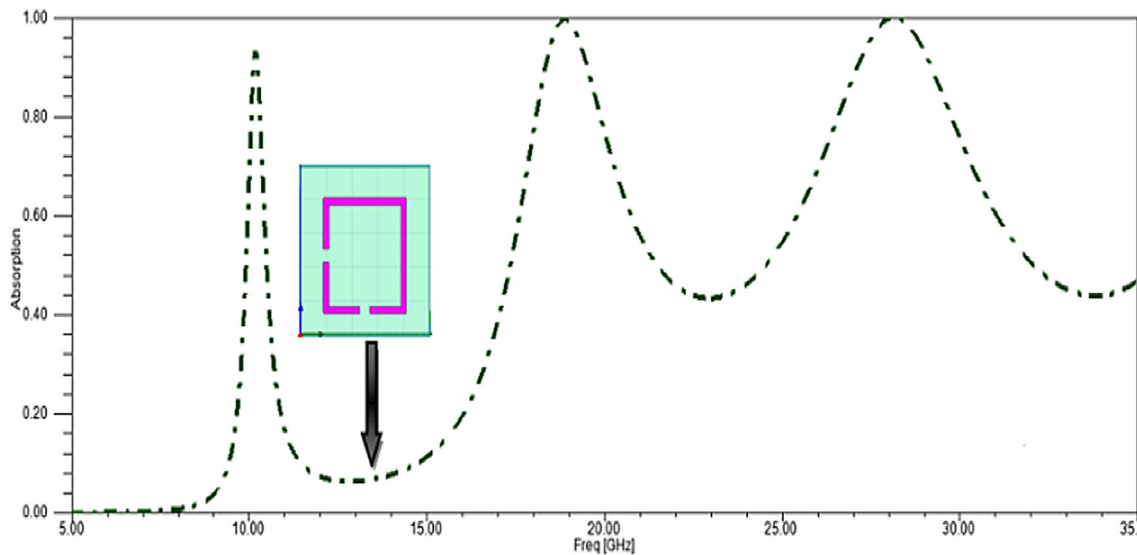


Figure 3. Absorption ratio vs. frequency of inner SSR.

Calculating the electromagnetic field surface current distribution of the MA is the first step in determining the absorption process. Figure 6 designates the current density distribution on top of the surface at resonant frequencies. At 10.40 GHz, the concentration of current is exposed more on the (SSR)_i, whereas at 12.80 GHz, the concentration of current is more on the (SSR)_o (figure 7).

3.2 Experimental studies

A prototype of the proposed PMA was fabricated in the laboratory with a 10×10-unit cell structure array with an overall dimension of 50 x 50 mm², as shown in figure 8, whereas a single-unit cell structure is 5 × 5 mm². An experimental setup for the proposed prototype measurement is shown in figure 9. In this setup; two horn antennas

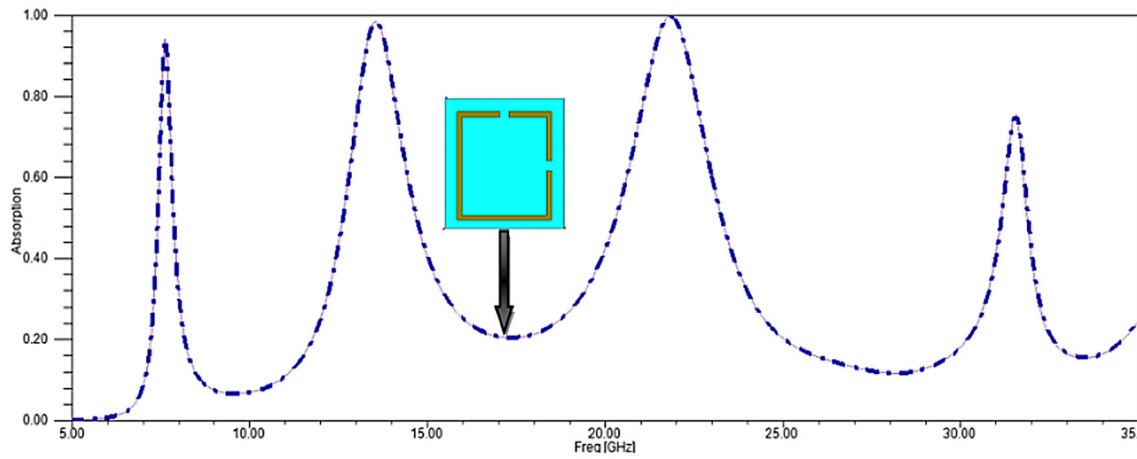


Figure 4. Absorption ratio vs. frequency of outer SSR.

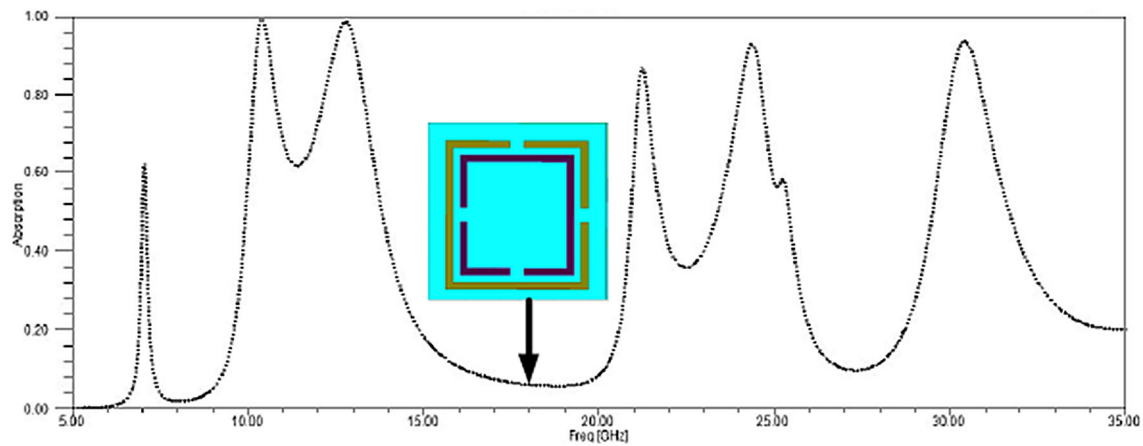


Figure 5. Absorption ratio vs. frequency graph of DSSR.

Table 2. Absorption effectiveness over a different geometry structure.

Geometry	Peak 1	Peak 2	Peak 3	Peak 4
Inner SSR (SSR) _i				
Frequency (GHz)	10.19	18.92	28.16	–
Absorption ratio (%)	93.04	99.58	99.99	–
Outer SSR(SSR) _o				
Frequency (GHz)	7.64	13.60	21.89	31.57
Absorption ratio (%)	93.30	98.11	99.54	74.66

have been used, from which one is used for the transmission of EM waves and the other one is used for receiving the same.

The obtained experimental results for the PMA are presented in figure 10 and compared with the simulated result. Table 3 shows the measured and simulated resonance peak frequency of the designed PMA. It contains a listing of the relative error that resulted from the simulation and measurement, which is less than 2%.

Table 3. Relative error between measured and simulated frequency.

Peaks	Measured frequency F_M (GHz)	Simulated frequency F_S (GHz)	Relative error $E_i = \frac{F_m - F_s}{F_m} \times 100\%$
1	10.386	10.273	1.0880%
2	13.000	12.800	1.5384%
3	20.880	21.050	-0.8141%
4	23.873	24.290	-1.7467%
5	30.030	30.410	-1.2654%

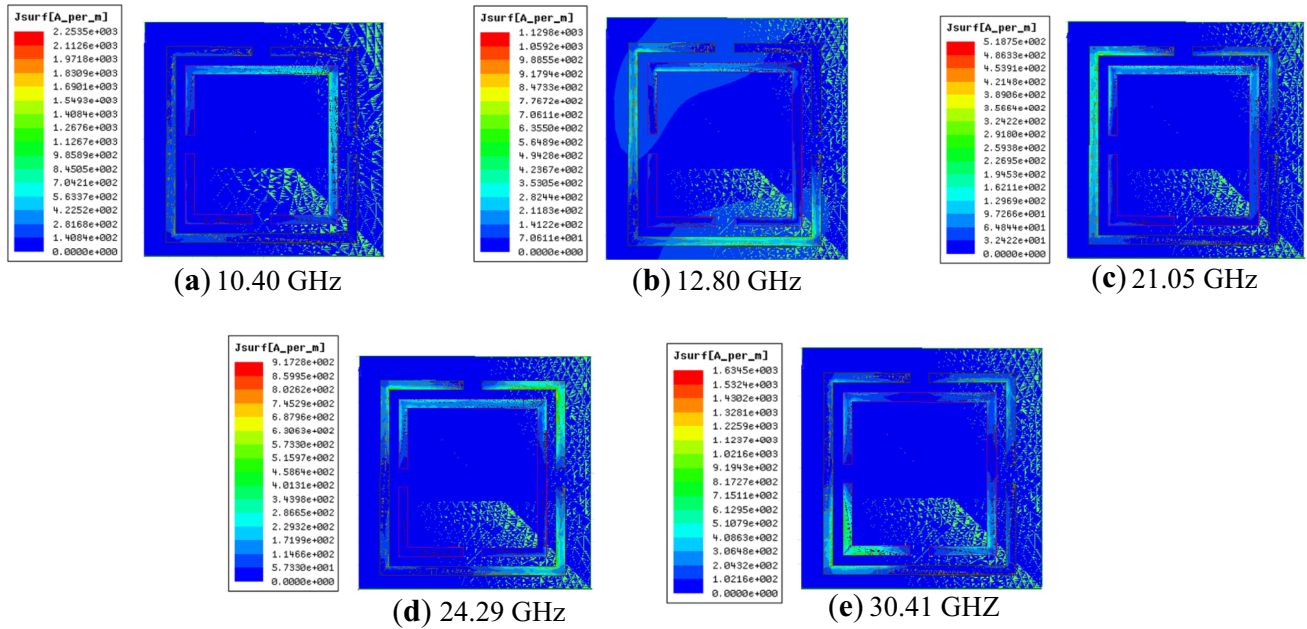


Figure 6. Current density plot of the proposed unit cell at (a) 10.40 GHz (b) 12.80 GHz (c) 21.05 GHz (d) 24.29 GHz (e) 30.41GHz.

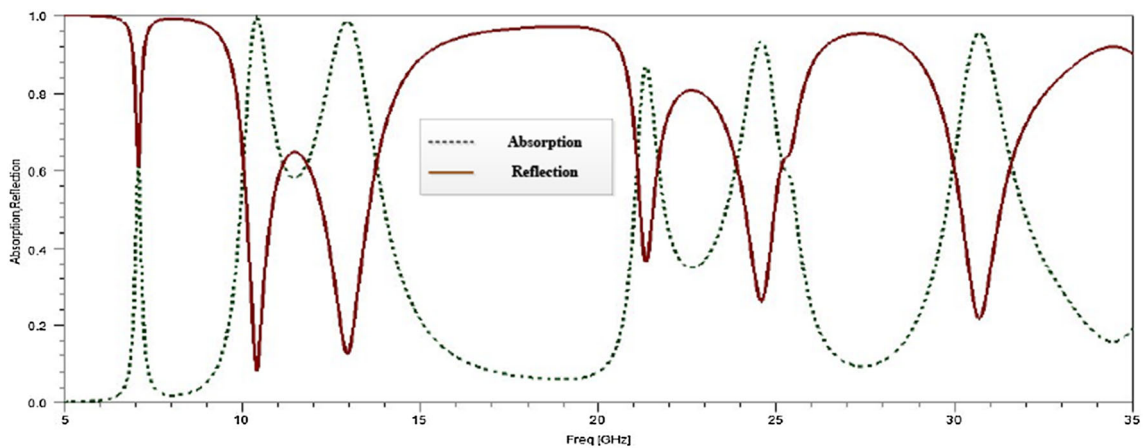


Figure 7. Absorption and reflection vs frequency graph of novel DSSR absorber.

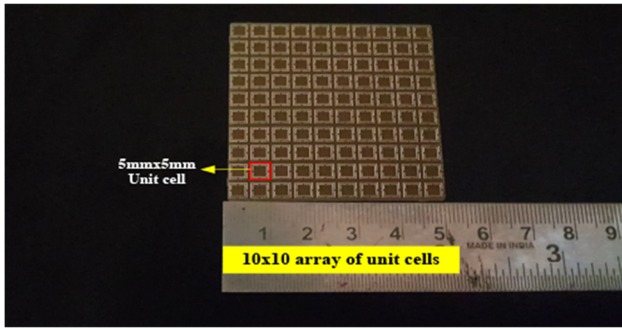


Figure 8. Fabricated prototype of 10×10 array unit cell structure.

3.3 Comparison of novel absorber with existing absorbers

Table 4 demonstrates how the proposed work compares against existing MAs. It is found that when the mechanism analysis and simulation results are compared, the absorption performance is quite good, with a very compact size unit cell.

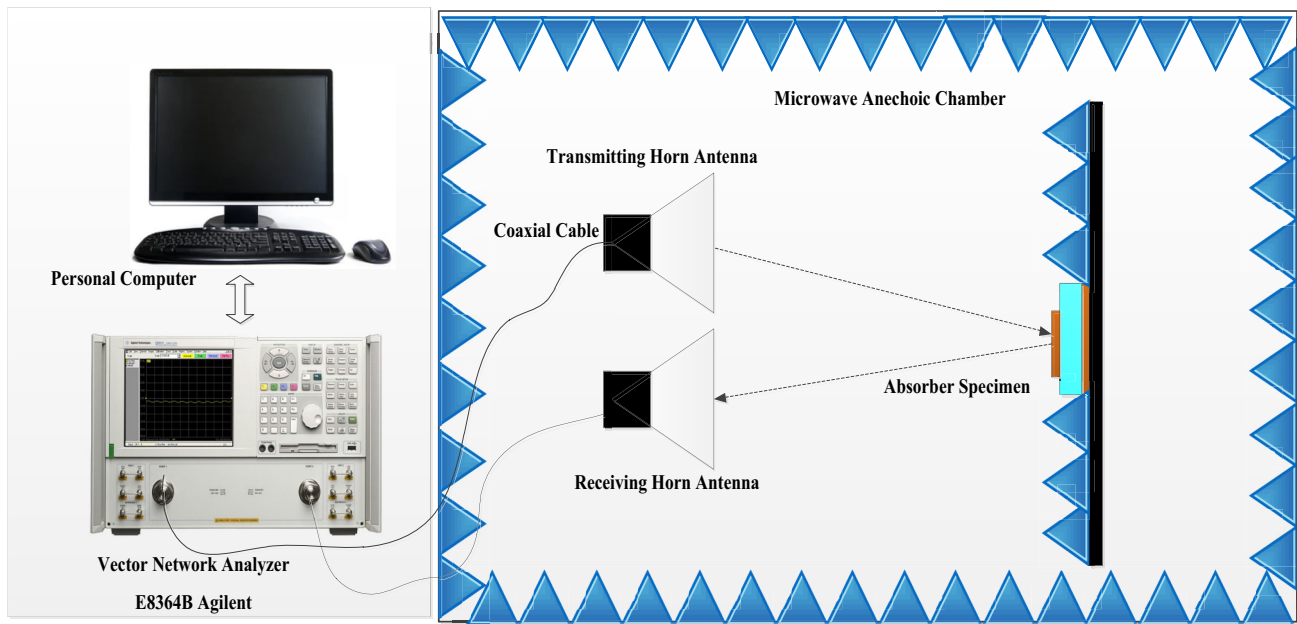


Figure 9. Block diagram of anechoic chamber testing setup.

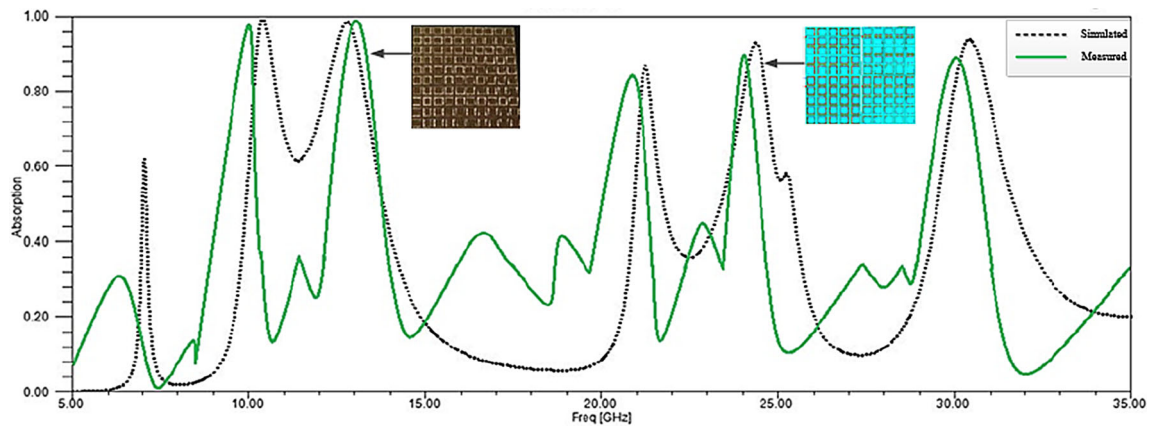

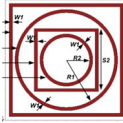
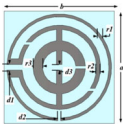

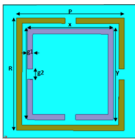


Figure 10. The simulated and measured result of the novel DSSR absorber.

Table 4. Comparison between the existing MAs and proposed work magnetic Properties

Related research	Design of top layers	Structure	Material	Absorption frequency	Thickness	Absorptivity	Size (mm)
[12]	Square with spiral symmetric		Copper	8.5GHz 13.5GHz 17GHz	0.4 mm	99.9% 99.5% 99.9%	8×8
[13]	Double square rings and double circle rings		Copper Clad	3.1GHz 5.4GHz 7.6GHz 10.98GHz	1.6 mm	92% 97% 90% 90%	12×12
[14]	Circular split ring resonator		Copper FR4	4.1GHz 6.86GHz 11.3GHz 13.45GHz	1.5 mm	97.9% 99.1% 99.5% 99.95%	8×8
[15]	Rectangular frame outside the Buddhist logo		FR4	5.24GHz 8.84GHz 14.28GHz 15.96GHz 18.60GHz	1.2 mm	96.39% 98.13% 98.26% 98.07% 99.75%	15.5×15.5
Proposed	Dual split square metal resonator (DSSR)		FR4	10.40GHz 12.80GHz 21.05GHz 24.29GHz 30.41GHz	1 mm	99.99% 98.44% 86.78% 92.74% 93.65%	5×5

4. Conclusion

In this paper, a novel DSSR penta-band metamaterial absorber operating in the microwave spectrum was proposed in the microwave range. The proposed work has been carefully designed with a compact size of 5 mm×5 mm and substrate thickness of 1 mm for a pentaband metamaterial absorber with good absorptivity. According to the results, the novel DSSR MA has five resonance peaks, and the absorption peaks may be found at the resonance frequencies of 10.40 GHz, 12.80 GHz, 21.05 GHz, 24.29 GHz, and 30.41 GHz with absorption peaks of 99.99%, 98.44%, 86.78%, 92.74%, and 93.65% respectively between simulated and measured findings is less than 2%.

References

[1] Mishra Kumar R, Gupta Dutt R and Datar S 2021 Metamaterial Microwave Absorber (MMA) for Electromagnetic Interference (EMI) Shielding in X-Band. *Plasmonics*. 16(6): 2061–2071.

[2] Ramachandran T, Faruque M, Ahamed E and Abdullah S 2019 Specific absorption rate reduction of multi split square ring etamaterial for L- and S-band application. *Results Phys*. 15(6): 102668

[3] Smolyaninov I and Smolyaninova V 2018 *Metamaterial superconductors*. *Nanophotonics*. 7(5): 795–818

[4] Haxha S, AbdelMalek F and Ouerghi F *et al.* 2018 2018 Metamaterial Superlenses Operating at Visible Wavelength for Imaging Applications. *Scientific Report*. 8(1): 1–15

[5] Zhong J, Huang H, Wen G, Sun H and Zhu Z 2012 The Design and Applications of Tunable Metamaterials. *Procedia Engineering*. 29: 802–807

[6] Bala B, Rahim M, Murad N, Ismail M and Majid H 2012 Design and analysis of metamaterial antenna using Triangular resonator. *Asia-Pacific Microw. Conf. Proceedings, APMC*. 2014, pp. 577–579

[7] Md Ali Adlina S, Abu M and Zabri Normi S 2020 A review: The development of metamaterial absorber. *Int. J. Integr. Eng.* 12(1): 72–80

[8] Mulla B and Sabah C 2017 Multi-band metamaterial absorber topology for infrared frequency regime. *Phys. E Low-dimensional Syst. Nanostructures*. 86: 44–51

[9] Zhang Y, Yi Z and Wang X *et al.* 2021 Dual band visible metamaterial absorbers based on four identical ring patches. *Phys. E Low-dimensional Syst. Nanostructures* 127: 114526

[10] Garg P and Jain P 2020 Novel ultrathin penta-band metamaterial absorber. *AEU - Int. J. Electron. Communication*. 116: 153063

[11] Varadhan C 2021 S Arulselvi and F Ashine Chamatu 2021 Effects of the FR 4 Substrate Realized in a Circularly Polarized UHF-RFID Reader Antenna with Fractal Geometry for Enhancing Parameters *Adv. Mater. Sci. Eng.* 2021: 865–867

- [12] Deng G, Lv K, Sun H and Yang J *et al* 2020 An Ultrathin, Triple-Band Metamaterial Absorber with Wide-Incident-Angle Stability for Conformal Applications at X and Ku Frequency Band. *Nanoscale Res. Lett.*, 15(1)
- [13] Kalraiya S, Chaudhary R, and Gangwar R 2019 Compact quad-band polarization independent metamaterial absorber using circular/square metallic ring resonator. *Materials Research Express*. vol. 6
- [14] Moniruzzaman M, Islam M, Muhammad G, Singh Jeet M and Samsuzzaman M 2020 Quad band metamaterial absorber based on asymmetric circular split ring resonator for multiband microwave applications. *Results Phys.* 19(10): 103467
- [15] Wu H, Ji S, Zhao S, Luo S and Dai H 2022 Design and analysis of a five-band metamaterial absorber. *J. Electromagn. Waves Appl.* 36(9): 1273–1284